

Why case fatality ratios can be misleading: individual- and population-based mortality estimates and factors influencing them

Lucas Böttcher¹, Mingtao Xia², and Tom Chou^{1,2,3}

¹*Dept. of Computational Medicine, UCLA, Los Angeles, CA 90095-1766*

²*Dept. of Mathematics, UCLA, Los Angeles, CA 90095-1555 and*

³*Beijing Computational Science Research Center, Beijing, China*

Different ways of calculating mortality ratios during epidemics have yielded very different results, particularly during the current COVID-19 pandemic. We formulate both a survival probability model and an associated infection duration-dependent SIR model to define individual- and population-based estimates of dynamic mortality ratios. The key parameters that affect the dynamics of the different mortality estimates are the incubation period and the time individuals were infected before confirmation of infection. We stress that none of these ratios are accurately represented by the often misinterpreted case fatality ratio (CFR), the number of deaths to date divided by the total number of confirmed infected cases to date. Using data on the recent SARS-CoV-2 outbreaks, we estimate and compare the different dynamic mortality ratios and highlight their differences. Informed by our modeling, we propose more systematic methods to determine mortality ratios during epidemic outbreaks and discuss sensitivity to confounding effects and uncertainties in the data.

INTRODUCTION

The mortality ratio is a key metric describing the severity of a viral disease [1]. These metrics typically change in time before converging to a constant value and can be defined in a number of ways. One commonly used metric is the (confirmed) case fatality ratio (CFR or cCFR), the total number of deaths to date, $D(t)$, divided by the total number of all confirmed cases to date $N(t)$ [1–4]. Infection fatality ratios (IFR), the number of deaths to date divided by the number of all infecteds, have also been used [5–7] although the IFR requires an estimate of the number of unconfirmed infecteds.

Both the CFR and IFR have been widely estimated from aggregated population data from past outbreaks [2] as well as from those of the recent SARS-CoV-2 outbreaks [1, 5, 7–11]. We show examples of CFR curves in Fig. 1 and in the *Supplemental Information* (SI). As of March 31, 2020, the global $\text{CFR}(t) = D(t)/N(t) = 42,158/858,892 \approx 4.9\%$ [12], while CFRs in individual regions vary significantly. Clearly, this estimate would correspond to the actual mortality ratio if (i) all infecteds were tested and (ii) *all* remaining unresolved individuals recover. However, some infected patients will die, increasing the estimated mortality ratio over time. Despite the underestimation of this type of population-based measurement, it is still commonly being used by various health officials and is often inconsistently defined as $\text{deaths}/(\text{deaths} + \text{recovereds})$ even though this difference has been clearly distinguished [13].

During the severe 2003 acute respiratory syndrome (SARS) outbreak in Hong Kong, the World Health Organization (WHO) also used the aforementioned estimate to obtain a CFR of 4.5% while the final values, after resolution of infecteds, approached 17.0% [15, 16]. For the ongoing SARS-CoV-2 outbreaks, analyses by WHO and many others still use the $\text{CFR} = D(t)/N(t)$ metric [7, 9, 11], (see Table I), or time-shifted variants [1, 6]. Since true mortality rates are critical for assessing the risks associated with epidemic outbreaks, typical underestimations by CFRs may lead to insufficient countermeasures and a more severe epidemic [17, 18].

An unambiguous definition of mortality ratio is the probability that a single, newly infected individual will eventually die of the disease. If there are sufficient individual-level or cohort data, these probabilities can be further stratified according to patient age, gender, health condition, etc. [1, 19]. This intrinsic mortality ratio, or probability of death, should be an *intrinsic* property of the virus and the infected individual, depending on age, health, access to health care, etc., and ought not *directly* depend on the population-level dynamics of infected and recovered individuals. Thus, it can be framed as a survival probability of a single infected individual. Whether this individual infects others does not directly affect his probability of eventually dying [20].

In the Results, we derive a model describing the probability $M_1(t)$ that an infected individual dies or recovers before time t . Importantly, these models incorporate the duration of infection (including an incubation period) before a patient tests positive at time $t = 0$. However, the CFR and other mortality measures are typically reported based on population data. Do these population-based measures, including CFR, provide reasonable measures of the probability of death of an individual? Also in the Results, we describe how mortality ratios are defined within population-level models, specifically, a disease duration-structured SIR model. We will show that population-based estimates are typically not a meaningful measure of mortality, but that under simplifying assumptions, the mortality ratio $M_p(t) = D(t)/(D(t) + R(t))$, where $R(t)$ is the number of recovereds up to time t , is more closely related to the true probability of death $M_1(t)$ [13]. The simplest population-level mortality ratio is currently (as of March 31, 2020)

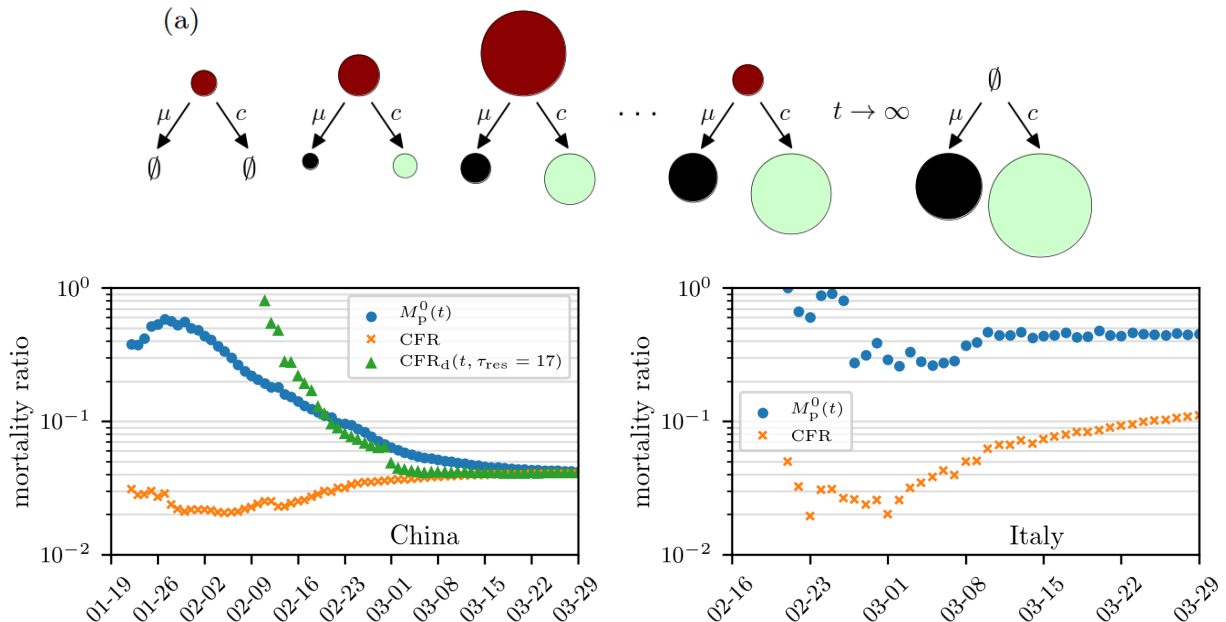


FIG. 1. **Mortality-ratio estimates.** (a) Evolution of the cumulative number of infected (red), death (black), and recovered (green) cases. The size of the circles indicates the number of cases in the respective compartments on a certain day. (b–c) Estimates of mortality ratios (see Eqs. (8) and (14)) of SARS-CoV-2 infections in China and Italy. The “delayed” mortality-ratio estimate CFR_d corresponds to the number of deaths to date divided by total number of cases at time $t - \tau_{res}$. Many studies use CFR_d , although this metric underestimates the individual-based mortality (defined below). Another population-based mortality ratio is $M_p^0(t)$, the number of deaths divided by the sum of death and recovered cases, up to time t . The data are based on Ref. [14].

| reference | CFR |
|--|------------------------|
| Xu <i>et al.</i> [3, 21] and Mahase [22] | 2% |
| Wu <i>et al.</i> [4] | 0.1-1% (outside Wuhan) |
| World Health Organization [23, 24] | 2-4% |
| Porcheddu <i>et al.</i> [25] | 2.3% (Italy and China) |
| Peeri [26] <i>et al.</i> | 2% |

TABLE I. Different CFR estimates of COVID-19.

42, 158/(42, 158 + 178, 100) \approx 19.1% [12], significantly higher than the March 31, 2020 $CFR \approx$ 4.9% estimate.

We use the same estimates for the rate parameters in our individual and population models to compute the different mortality ratios. Note that in general, both the individual mortality probability $M_1(t)$ and the population-based estimates $M_p(t)$ depend on the time of measurement t . By critically analyzing these estimates, the CFR, and a “delayed” case fatality ratio CFR_d , we illustrate and interpret the differences among these measures and discuss how changes or uncertainty in the data affect them. In the Discussion, we summarize our results and identify a correction factor to transform population-level mortality estimates into individual mortality probabilities.

RESULTS

Intrinsic individual mortality rate

Consider an individual that, at the time of positive testing ($t = 0$), had been infected for a duration τ_1 . A “survival” probability density can be defined such that $P(\tau, t|\tau_1)d\tau$ is the probability that the patient is still alive and infected (not recovered) at time $t > 0$ and has been infected for a duration between τ and $\tau + d\tau$. Since τ_1 is unknown, it must be estimated or averaged over some distribution. The individual survival probability evolves according to

$$\frac{\partial P(\tau, t|\tau_1)}{\partial t} + \frac{\partial P(\tau, t|\tau_1)}{\partial \tau} = -(\mu(\tau, t|\tau_1) + c(\tau, t|\tau_1))P(\tau, t|\tau_1), \quad (1)$$

where the death and recovery rates, $\mu(\tau, t|\tau_1)$ and $c(\tau, t|\tau_1)$, depend explicitly on the duration of infection at time t and implicitly on patient health and age a [27]. They may also depend explicitly on time t to reflect changes in clinical policy or available health care. For example, enhanced medical care may decrease the death rate μ , giving the individual's intrinsic physiological processes a chance to cure the patient.

If we assume an initial condition of one individual having been infected for time τ_1 at the time of confirmation, Eq. 1 can be solved using the method of characteristics (see the SI). From the solution $P(\tau = t + \tau_1, t|\tau_1)$ (see the *Methods*) one can derive the probabilities of death and recovery by time t as

$$P_d(t|\tau_1) = \int_0^t ds \mu(\tau_1 + s, s)P(\tau_1 + s, t|\tau_1), \quad P_r(t|\tau_1) = \int_0^t ds c(\tau_1 + s, s)P(\tau_1 + s, t|\tau_1). \quad (2)$$

The probability that an individual died before time t , conditioned on resolution (either death or recovery), is then defined as

$$M_1(t|\tau_1) = \frac{P_d(t|\tau_1)}{P_d(t|\tau_1) + P_r(t|\tau_1)}. \quad (3)$$

Equations (2) and (3) also depend on all other relevant patient attributes such as age, accessibility to health care, etc. In the long-time limit, when resolution has occurred ($P_d(\infty) + P_r(\infty) = 1$), the individual mortality ratio is simply $M_1(\infty) = P_d(\infty)$. In order to capture the dependence of death and recovery rates on the time an individual has been infected, we propose a constant recovery rate c and a piece-wise constant death rate $\mu(\tau|\tau_1)$ that is not explicitly a function of time t :

$$c(\tau, t|\tau_1) = c, \quad \mu(\tau|\tau_1) = \begin{cases} 0 & \tau \leq \tau_{\text{inc}} \\ \mu_1 & \tau > \tau_{\text{inc}} \end{cases}, \quad (4)$$

where τ_{inc} is the incubation time during which the patient is asymptomatic, has zero death rate, but can recover by clearing the virus. In other words, some patients fully recover without ever developing serious symptoms.

For coronavirus infections, the incubation period appears to be highly variable with a mean of $\tau_{\text{inc}} \approx 6.4$ days [29]. We can estimate μ_1 and c using individual patient data where 19 patients (outside Hubei) had been tracked from the date on which their first symptoms occurred until the disease resolved [28].

Two out of 19 patients died, on average, 20.5 days after first symptoms occurred and the mean recovery time of the remaining 17 patients is 16.8 days. We show the recovery-time distribution in Fig. 2(a). Since we know that the mortality ratio in this dataset is 2/19, we can determine the dependence between μ_1 and c according to $\mu_1/(\mu_1 + c) \approx 2/19$ (or $c/\mu_1 \approx 8.5$). The constant recovery and after-incubation period death rates [30] are estimated to be

$$c = \frac{1}{20.5}/\text{day} \approx 0.049/\text{day} \quad \text{and} \quad \mu_1 = c/8.5 \approx 0.006/\text{day}. \quad (5)$$

Using these numbers, the recovery and death rate functions $c(\tau, t|\tau_1)$ and $\mu(\tau|\tau_1)$ are plotted as functions of τ in Fig. 2(b). We show the evolution of $M_1(t|\tau_1)$ at different values of τ_1 in Fig. 2(c). The corresponding long-time limit $M_1(\infty)$ is readily apparent in Fig. 2(d): for $\tau_1 \geq \tau_{\text{inc}}$, $M_1(\infty) = \mu_1/(\mu_1 + c) \approx 0.105$, while $M_1(\infty) < \mu_1/(\mu_1 + c)$ when $\tau_1 < \tau_{\text{inc}}$. The smaller expected mortality associated with early identification of infection arises from the remaining incubation time during which the patient has a chance to recover without possibility of death. When conditioned on testing positive at or after the incubation period, the patient immediately suffers a positive death rate, increasing his $M_1(\infty)$.

Finally, in order to infer M_1 (and also indirectly μ and c) during an outbreak, a number of statistical issues must be considered. First, if the outbreak is ongoing, there may not be sufficient long-time cohort data. Second, τ_1 is unknown. Since testing typically occurs at the onset of symptoms, most positive patients will have been infected a few days earlier. The uncertainty in τ_1 can be represented by a probability density $\rho(\tau_1)$ for the individual. The expected mortality can then be constructed as an average over $\rho(\tau_1)$:

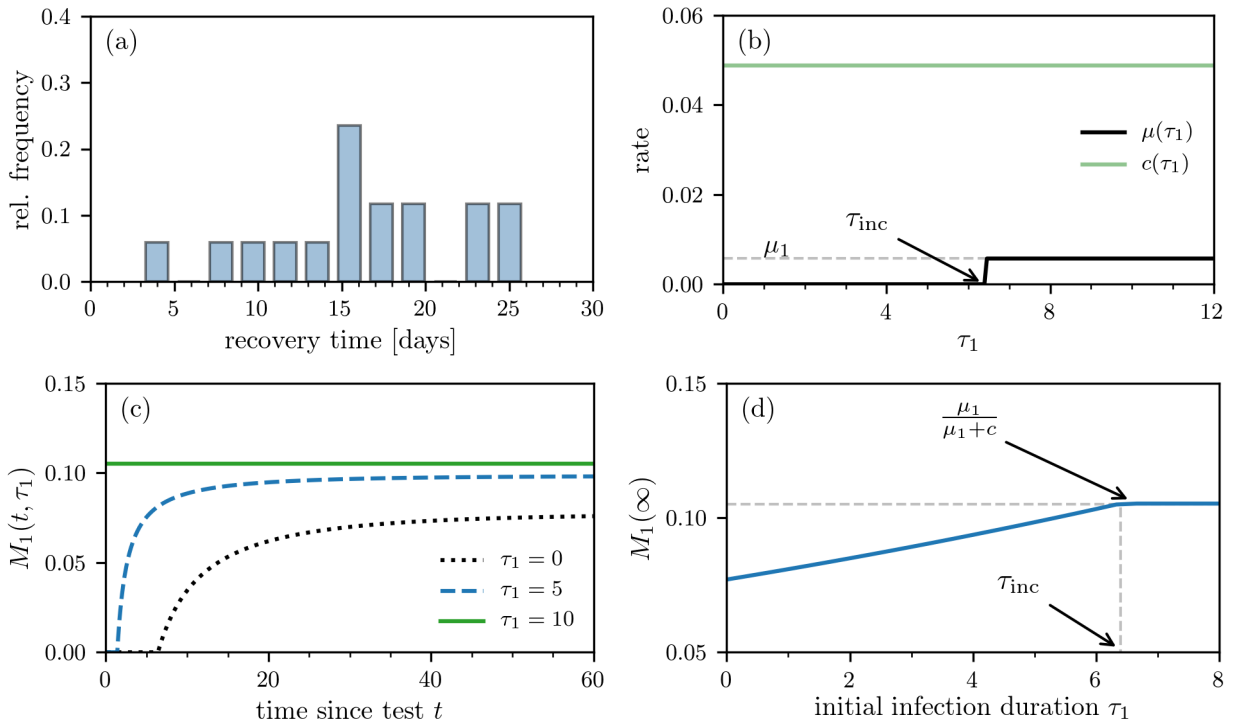


FIG. 2. **Individual mortality ratio.** (a) Recovery time after first symptoms occurred based on individual data of 17 patients [28]. (b) Death- and recovery rates as defined in Eq. (4). The death rate $\mu(\tau_1)$ approaches μ_1 for $\tau_1 > \tau_{\text{inc}}$, where τ_{inc} is the incubation period and τ_1 is the time the patient has been infected before first being tested positive. (c) The individual mortality ratio $M_1(t|\tau_1)$ for $\tau_{\text{inc}} = 6.4$ days at different values of τ_1 . Note that the individual death probability $P_d(t|\tau_1)$ and $M_1(t|\tau_1)$ are nonzero only after $t > \tau_{\text{inc}} - \tau_1$. (d) The asymptotic individual mortality ratio $M_1(\infty)$ (see Eq. (3)) as a function of τ_1 .

$$\bar{M}_1(t) = \frac{\bar{P}_d(t)}{\bar{P}_d(t) + \bar{P}_r(t)}, \quad (6)$$

where $\bar{P}_d(t)$ and $\bar{P}_r(t)$ are the τ_1 -averaged probabilities death and cure probabilities.

Some properties of the distribution $\rho(\tau_1)$ can be inferred from the behavior of patients. Before symptoms arise, only very few patients will know they have been infected, seek medical care, and get their case confirmed (*i.e.*, $\rho(\tau_1) \approx 0$ for $\tau_1 \approx 0$). The majority of patients will contact hospitals/doctors when they have been infected for a duration of τ_{inc} . The distribution $\rho(\tau_1)$ thus reaches its maximum near or shortly after τ_{inc} . Since patients are most likely to test positive after experiencing symptoms, we choose a gamma distribution

$$\rho(\tau_1; n, \gamma) = \frac{\gamma^n}{\Gamma(n)} \tau_1^{n-1} e^{-\gamma\tau_1} \quad (7)$$

with shape parameter $n = 8$ and rate parameter $\gamma = 1.25/\text{day}$ so that the mean n/γ is equal to $\tau_{\text{inc}} = 6.4$.

Upon using the rates in Eqs. (4) and averaging over $\rho(\tau_1)$, we derived expressions for $\bar{P}(t)$, $\bar{P}_d(t)$, and $\bar{P}_r(t)$ which are explicitly given in the SI. Using the values in Eq. (5) we find an expected individual mortality ratio $\bar{M}_1(t)$ (which are subsequently plotted in Fig. 3) and its asymptotic value $\bar{M}_1(\infty) = \bar{P}_d(\infty) = 0.101$. Of course, it is also possible to account for more complex time-dependent forms of c and μ_1 [31], but we will primarily use Eqs. (4) in our subsequent analyses.

In the next section, we define population-based estimates for mortality ratios, $M_p(t)$, and explore how they can be computed using SIR-type models. By comparing $M_1(t)$ to $M_p(t)$, we gain insight into whether population-based metrics are good proxies for individual mortality ratios. We will outline the mathematical differences and additional errors that confound population-level estimates.

Infection duration-dependent SIR model

While individual mortalities can be estimated by tracking many individuals from infection to recovery or death, oftentimes, the available data are not resolved at the individual level and only total populations are given. Typically, one has the total number of cases accumulated up to time t , $N(t)$, the number of deaths to date $D(t)$, and the number of cured/recovered patients to date $R(t)$ (see Fig. 1). The CFR is simply $D(t)/N(t)$. Note that $N(t)$ includes unresolved cases and that $N(t) \geq R(t) + D(t)$. Resolution (death or recovery) of all patients, $N(\infty) = R(\infty) + D(\infty)$, occurs only well after the epidemic passes.

A variant of the CFR commonly used in the literature [3, 4] is the delayed CFR

$$\text{CFR}_d(t, \tau_{\text{res}}) = \frac{D(t)}{N(t - \tau_{\text{res}})}, \quad (8)$$

where τ_{res} is a corresponding time lag that accounts for the duration from the day when first symptoms occurred to the day of cure/death. Many estimates of the COVID-19 mortality ratio assume that $\tau_{\text{res}} = 0$ [3, 4] and thus underestimate the number of death cases $D(t)$ that result from a certain number of infected individuals. Similar underestimations using CFR_d have been reported in previous epidemic outbreaks of SARS [13, 15] and Ebola [32].

Alternatively, a simple and interpretable population-level mortality ratio is $M_p(t) = D(t)/(R(t) + D(t))$, the death ratio of all *resolved* cases. To provide a concrete model for $D(t)$ and $R(t)$, and hence $M_p(t)$, we will use a variant of the standard infection duration-dependent susceptible-infected-recovered (SIR)-type model described by [33]

$$\begin{aligned} \frac{dS(t)}{dt} &= -S(t) \int_0^\infty d\tau' \beta(\tau', t) I(\tau', t), \\ \frac{\partial I(\tau, t)}{\partial t} + \frac{\partial I(\tau, t)}{\partial \tau} &= -(\mu(\tau, t) + c(\tau, t)) I(\tau, t), \end{aligned} \quad (9)$$

and $dR(t)/dt = \int_0^\infty d\tau c(\tau, t) I(\tau, t)$, where $S(t)$ is the number of susceptibles, $I(\tau, t)$ is density of individuals at time t who have been infected for time τ , and $R(t)$ is the number of recovered individuals. The rate at which an individual infected for time τ at time t transmits the infection to a susceptible is denoted by $\beta(\tau, t)S(t)$. For simplicity, we assume only community spread and neglect immigration of infected, which can be straightforwardly incorporated [33].

Note that the equation for $I(\tau, t)$ is identical to the equation for the survival probability described by Eq. (1). It is also equivalent to McKendrick age-structured models [34, 35] [36]. Infection of susceptibles is described by the boundary condition

$$I(\tau = 0, t) = S(t) \int_0^\infty d\tau' \beta(\tau', t) I(\tau', t), \quad (10)$$

which is similar to that used in age-structured models to represent birth [34]. Finally, we use an initial condition consistent with the infection duration density given by Eq. (7): $I(\tau, 0) = \rho(\tau; n = 8, \gamma = 1.25)$. Note that Eq. (10) assumes that all newly infected individuals are immediately identified; *i.e.*, these newly infected individuals start with $\tau_1 = 0$. After solving for the infected population density, the total number of deaths and recoveries to date can be found via

$$D_0(t) = \int_0^t dt' \int_0^\infty d\tau \mu(\tau, t') I(\tau, t'), \quad R_0(t) = \int_0^t dt' \int_0^\infty d\tau c(\tau, t') I(\tau, t'). \quad (11)$$

The corresponding total number of cases $N(t)$ in Eq. (8) is

$$N_0(t) = R_0(t) + D_0(t) + \int_0^\infty d\tau I(\tau, t). \quad (12)$$

In the definitions of $D_0(t)$, $R_0(t)$, and $N_0(t)$, we account for all possible death and recovery cases to date (see SI) and that newly infected individuals are immediately identified. We use these case numbers as approximations of the reported case numbers to study the evolution of mortality-ratio estimates. Mortality ratios based on these numbers underestimate the actual individual mortality M_1 (see the previous ‘‘Intrinsic individual mortality rate’’ subsection) since they involve individuals that have been infected for different durations τ , particularly recently infected individuals who have not yet died.

An alternative way to compute populations is to exclude the newly infecteds and consider only the initial cohort. The corresponding populations in this case are defined as

$$D_1(t) = \int_0^t dt' \int_{t'}^\infty d\tau \mu(\tau, t') I(\tau, t'), \quad R_1(t) = \int_0^t dt' \int_{t'}^\infty d\tau c(\tau, t') I(\tau, t'). \quad (13)$$

Since $D_1(t)$ and $R_1(t)$ do not include infecteds with $\tau < t$, they exclude the effect of newly infected individuals, but may yield more accurate mortality-ratios as they are based on an initial cohort of individuals in the distant past. The infections that occur after $t = 0$ contribute only to $I(\tau < t, t)$; thus, $D_1(t)$ and $R_1(t)$ do not depend on the transmission rate β , possible immigration of infecteds, or the number of susceptibles $S(t)$. Note that all the populations derived above implicitly average over $\rho(\tau_1; n, \gamma)$ for the first cohort of identified infecteds (but not subsequent infecteds). Moreover, the population density $I(\tau \geq t, t)$ follows the same equation as $\bar{P}(t|\tau_1)$ provided the same $\rho(\tau_1; n, \gamma)$ is used in their respective calculations.

The two different ways of partitioning populations (Eqs. (11) and (13)) lead to two different population-level mortality ratios

$$M_p^0(t) = \frac{D_0(t)}{D_0(t) + R_0(t)} \quad \text{and} \quad M_p^1(t) = \frac{D_1(t)}{D_1(t) + R_1(t)}. \quad (14)$$

Since the populations $D_0(t)$ and $R_0(t)$, and hence $M_p^0(t)$, depend on disease transmission through $\beta(\tau, t)$ and $S(t)$, we expect $M_p^0(t)$ to carry a different interpretation from $M_1(t)$ and $M_p^1(t)$.

In the special case in which μ and c are constants, the time-integrated populations $\int_0^t dt' \int_0^\infty d\tau I(\tau, t')$ and $\int_0^t dt' \int_{t'}^\infty d\tau I(\tau, t')$ factor out of $M_p^0(t)$ and $M_p^1(t)$, rendering them time-independent and

$$M_p^{0,1} = \frac{\mu_1}{\mu_1 + c} = M_1. \quad (15)$$

Thus, only in the special time-homogeneous case do both population-based mortality ratios become *independent* of the population (and transmission β) and coincide with the individual death probability.

To illustrate the differences between $M_1(t)$, $M_p^{0,1}(t)$, and $\text{CFR}_d(t, \tau_{\text{res}})$ in more general cases, we use the simple death and cure rate functions given by Eqs. (4) in solving Eqs. (1) and (9). For $\beta(\tau, t)$ in Eq. (10), we account for incubation effects by neglecting transmission during the asymptomatic incubation period ($\tau \leq \tau_{\text{inc}}$) and assume

$$\beta(\tau, t) = \begin{cases} 0 & \tau \leq \tau_{\text{inc}} \\ \beta_1 & \tau > \tau_{\text{inc}}. \end{cases} \quad (16)$$

We use the estimated basic reproductive number $\mathcal{R}_0 = \beta_1 S(0)/(\mu_1 + c) \approx 2.91$ [29] to fix $\beta_1 S(0) = (\mu_1 + c)\mathcal{R}_0 \approx 0.158/\text{day}$. We also first assume that the susceptible population does not change appreciably before quarantine and set $S(t) = S(0)$. Thus, we only need to solve for $I(\tau, t)$ in Eqs. (9) and (10). We solve Eqs. (9) and (10) numerically (see the *Methods* section for further details) and use these numerical solutions to compute $D_{0,1}(t)$, $R_{0,1}(t)$, and $N_{0,1}(t)$ (see Fig. 3(a) and (b)), which are then used in Eqs. (14) and $\text{CFR}_d(t - \tau_{\text{res}})$. To determine a realistic value of the time lag τ_{res} , we use data on death/recovery periods of 36 tracked patients [28] and find that patients recover/die, on average, $\tau_{\text{res}} = 16.5$ days after first symptoms occurred.

We show in Figs. 3(c) and (d) that $M_p^1(t)$ approaches the individual mortality ratio $\bar{M}_1(\infty) \approx 0.1$ given in the ‘‘Intrinsic individual mortality rate’’ subsection above. This occurs because the model for $P(\tau, t)$ and $I(\tau, t)$ are equivalent and we assumed the same initial distribution $\rho(\tau; 8, 1.25)$ for both quantities. However, the population-level mortality ratios $\text{CFR}_d(t, \tau_{\text{res}})$ and $M_p^0(t)$ also take into account recently infected individuals who may recover before symptoms. This difference yields different mortality ratios because newly infecteds are implicitly assumed to be detected immediately and all have $\tau_1 = 0$. Thus, the underlying infection-time distribution is not the same as that used to compute $\bar{M}_p^1(t)$ (see the SI for further details). The mortality ratios $\text{CFR}_d(t, \tau_{\text{res}})$ and $M_p^0(t)$ should not be used to quantify the individual mortality probability of individuals who tested positive. Moreover, due to evolution of the disease, $D(t)$, $R(t)$, and $N(t)$ do not change with the same rates during an outbreak, the population-level mortality measures $\text{CFR}_d(t, \tau_{\text{res}})$ and $M_p^0(t)$ reach their final steady state values only after sufficiently long times (see Fig. 3(c) and (d)).

The evolution of the mortality ratios in Fig. 3 qualitatively resembles the behavior of the mortality-ratio estimates in Fig. 1. As shown in Fig. 1, the population-based estimates for coronavirus varies, decreasing in time for China but fluctuating for Italy. These changes could result from changing practices in data collecting, or from explicitly time-inhomogeneous parameters $\mu(\tau, t)$, $c(\tau, t)$, and/or $\beta(\tau, t)$.

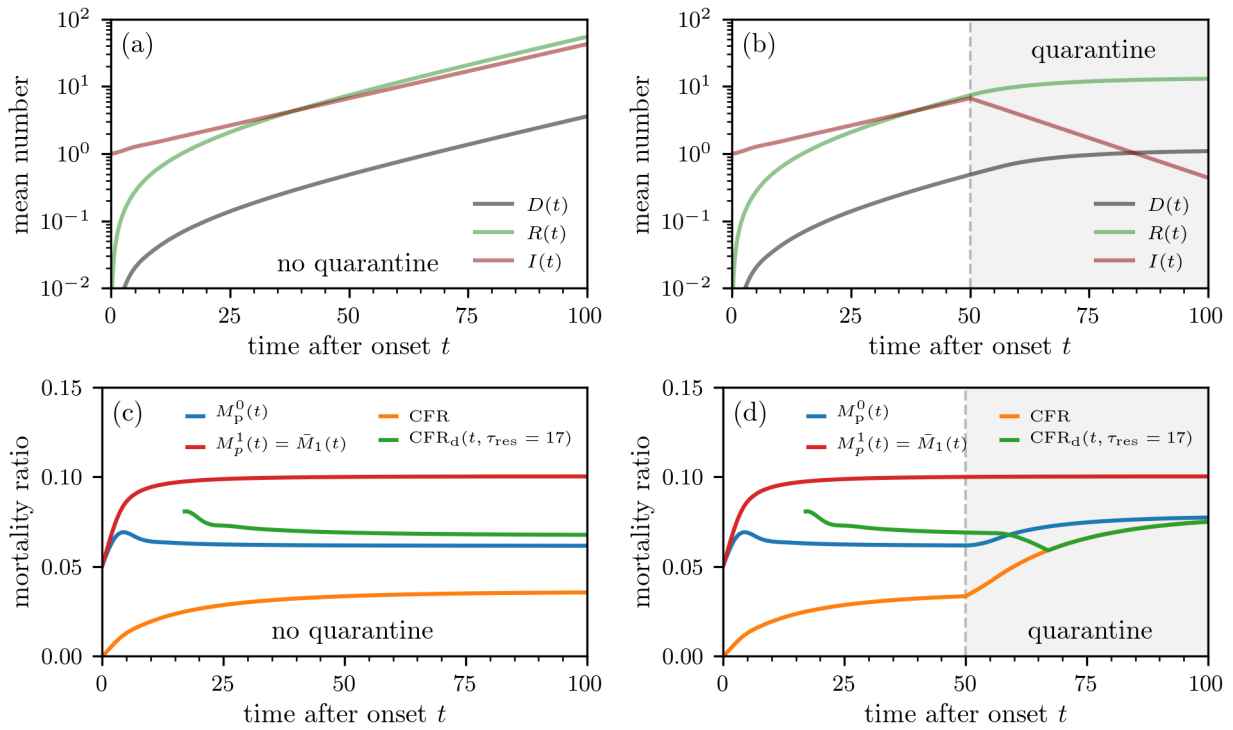


FIG. 3. **Population-level mortality-ratio estimates.** Outbreak evolution and mortality ratios without containment measures (a,c) and with quarantine (b,d). The curves are based on numerical solutions of Eqs. (9) using the initial condition $I(\tau, 0) = \rho(\tau; 8, 1.25)$ (see Eq. (7)). The death and recovery rates are defined in Eqs. (4) and (5). We use a constant infection rate $\beta_1 S(0) = 0.158/\text{day}$, which we estimated from the basic reproduction number of SARS-CoV-2 [29]. To model quarantine effects, we set $\beta_1 = 0$ for $t > 50$. We show the mortality-ratio estimates $M_p^0(t)$ and $M_p^1(t)$ (see Eq. (14)) and $\text{CFR}_d(t, \tau_{\text{res}})$ (see Eqs. (8), (11), (12), and (14)).

Although population-level quarantining does not directly affect the individual mortality $M_1(t|\tau_1)$ or $\bar{M}_1(t)$, it can be easily incorporated into the SIR-type population dynamics equations through changes in $\beta(\tau, t)S(t)$. For example, we have set $S(t > t_q) = 0$ to represent implementation of a quarantine after $t_q = 50$ days of the outbreak. After $t_q = 50$ days, no new infections occur and the estimates $\text{CFR}_d(t, \tau_{\text{res}})$ and $M_p^0(t)$ start converging immediately towards their steady-state values (see Fig. 3(d)). Since the number of deaths decreases after the implementation of quarantine measures, the delayed $\text{CFR}_d(t, \tau_{\text{res}} = 17)$ is first decreasing until $t = t_q + \tau_{\text{res}} = 67$. For $t > 67$, the $\text{CFR}_d(t, \tau_{\text{res}} = 17)$ measures no new cases and is thus equal to the CFR.

DISCUSSION AND SUMMARY

During an epidemic, it is important to assess the severity of the disease by estimating its mortality and other disease characteristics. Assuming accurate data, the often-used CFR typically underestimates the true, final death ratio. For example, during the SARS outbreaks in Hong Kong, the WHO first estimated the fatality rate to 2.5% (March 30, 2003) whereas the final estimates reached values of about 17.0% (June 30, 2003) (see Fig. 4(a)) [16]. Standard metrics like the CFR are seen to be easily confounded by and sensitive to uncertainty in intrinsic disease parameters such as the incubation period and the time τ_1 a patient had been infected before clinical confirmation of infection. For the recent COVID-19 outbreaks, CFR-based measures may still provide reasonable estimates of the actual mortality across different age classes due to a counter-acting error in the numbers of unreported mild-symptom cases.

Here, we stress that more mechanistically meaningful and interpretable metrics can be defined and, as easily, estimated from population data as CFRs. Our proposed mortality ratios for viral epidemics are defined in terms of (i) individual survival probabilities and (ii) population ratios using numbers of deaths and recovered individuals. Both of these measures are based on the within-host evolution of the disease, and in the case of $M_p^{0,1}(t)$, the population-level transmission dynamics.

Among the metrics we describe, $M_p^1(t)$ is structurally closest to the individual mortality $\bar{M}_1(t)$ in that both are independent of disease transmission since new infections are not considered. Both of these mortality ratios converge

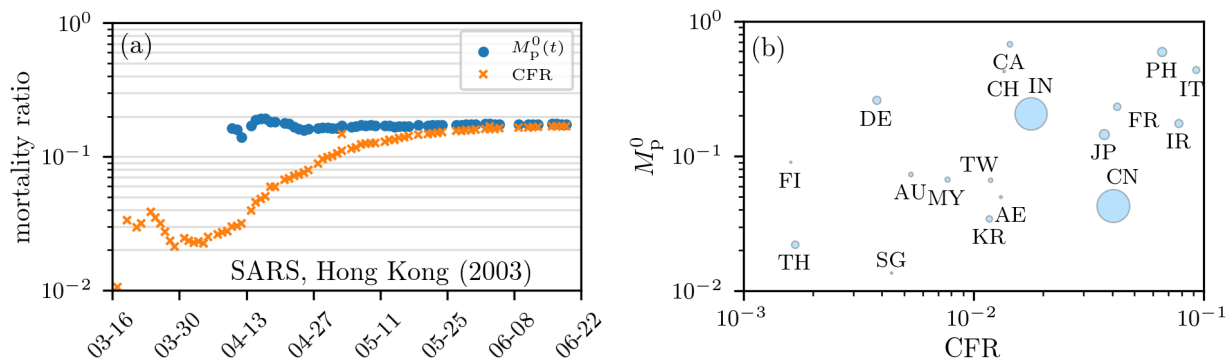


FIG. 4. **SARS mortality and region-dependence of COVID-19 mortality-ratio estimates.** (a) Estimates of mortality ratios (see Eqs. (8) and (14)) of SARS infections in Hong Kong (2003) [37]. (b) Mortality-ratio estimates of COVID-19 in different regions (see Eqs. (8) and (14) ($\tau_{\text{res}} = 0$)). We used data on the cumulative number of cases, recoveries, and deaths in Ref. [14] as of March 24, 2020. The marker sizes indicate the population of the corresponding countries. The metrics $M_p^0(t)$ and CFR are largely uncorrelated with correlation coefficient 0.33.

after an incubation time τ_{inc} to a value smaller than or equal to $\mu_1/(\mu_1 + c)$.

The most accurate estimates of M_1 can be obtained if we keep track of the fate of cohorts that were infected within a small time window in the past. By following only these individuals, one can track how many of them died as a function of time. As more cases arise, one should stratify them according to their estimated times since infection to gather improving statistics for $M_1(\infty)$. With the further spread of SARS-CoV-2 in different countries, data on more individual cases of death and recovery can be more easily stratified according to other central factors in COVID-19 mortality: age, sex, health condition.

Besides accurate cohort data, for which at present there are few for coronavirus, cumulative population data has been used to estimate the mortality ratio. The population-level metrics $M_p^0(t)$ and $\text{CFR}(t)$ implicitly depend on new infections and the transmission rate β . Despite this confounding factor, $M_p^0(t)$ and $\text{CFR}_d(t, \tau_{\text{res}})$ approach $e^{-c\tau_{\text{inc}}} \mu_1/(\mu_1 + c)$ as $t \rightarrow \infty$, where $e^{-c\tau_{\text{inc}}}$ is the probability that no recovery occurred during the incubation time τ_{inc} . Based on these results, we can establish the following connection between the different mortality ratios for initial infection times with distribution $\rho(\tau_1; n, \gamma)$ and mean $\bar{\tau} = n/\gamma$:

$$\text{CFR}_d(\infty) = M_p^0(\infty) \approx e^{-c\bar{\tau}} M_p^1(\infty) = e^{-c\bar{\tau}} \bar{M}_1(\infty). \quad (17)$$

According to Eq. (17), population-level mortality estimates (e.g., CFR and M_p^0) can be transformed, at least approximately, into individual mortality probabilities using the correction factor $e^{-c\bar{\tau}}$ with $\bar{\tau} \approx \tau_{\text{inc}}$.

Besides the mathematical differences between $M_1(t)$ and $M_p^0(t)$, CFR, estimating $M_p^0(t)$ and $\text{CFR}(t)$ from aggregate populations implicitly incorporate a number of confounding factors that contribute to their variability. In Fig. 4(b), we plot the population-level mortality-ratio estimates M_p^0 against the CFR for different regions and observe large variations and very little correlation between countries [38]. As of March 31, 2020, the value of M_p^0 in Italy is almost 45% and can increase further if the current conditions (e.g., treatment methods, age group proportion of infecteds, etc.) do not change. Differences between the mortality ratios in China and Italy (see Figs. 1(b) and (c)) might be a result of varying medical treatment strategies, different practices in data collecting (e.g., post-mortem testing), differences in the age demographics between the countries, and/or inaccuracies in reporting.

Even if the cohort initially tested was only a fraction of the total infected population, tracking $\bar{M}_1(t)$ or $M_p^1(t)$ of this cohort still provides an accurate estimation of the mortality rate. However, underreporting newly infecteds can confound CFR and $M_p^0(t)$. Current estimates show that only a minority of SARS-CoV-2 infections are reported (e.g., $f \approx 14\%$ in China before January 23, 2020) [39]. At early times (Fig. S2(a)) most patients, tested or untested, have not resolved. A reported/tested fraction $f < 1$ would not directly affect the CFRs or mortality ratios if the unreported/untested individuals die and recover in the same proportion as the tested infecteds (Fig. S2(b)). Undertesting would overestimate the true $M_p^0(t)$ and infection fatality ratio (IFR) if untested (presumably mildly or asymptomatic infected) individuals are less likely to die than the tested infecteds (Fig. S2(c)). If untested infecteds do not die at all, the true long-time mortality $\mathcal{M}_p^{0,1}(\infty) \approx f M_p^{0,1}(\infty)$ (see the SI). In the less likely scenario in which untested individuals do not receive medical care and hence die at a faster rate than tested patients (see Fig. S2(d)), $M_p^0(\infty)$ and CFR based on the tested fraction would underestimate the true long-time mortality $\mathcal{M}_p^{0,1}(\infty)$ and IFR, respectively.

Besides underreporting, the delay in transmission after becoming infected will also affect $M_p^0(t)$. Although we have assumed that transmission occurs only after the incubation period when symptoms arise, there is evidence of asymptomatic transmission of coronavirus [39, 40]. Asymptomatic transmission can be modeled by setting $\beta(\tau) > 0$ even for $\tau < \tau_{inc}$. An undelayed transmission in a no-quarantine scenario causes relatively more new infecteds who have not had the chance to die yet, leading to a *smaller* mortality ratio $M_p^0(t)$. Within our SIR model, delaying transmission reduces the number of infected individuals and deaths at any given time but *increases* the measured mortality ratio $M_p^0(t)$. Without quarantine, the asymptotic values $M_p^0(\infty)$ and $CFR(\infty)$ will also change as a result of changing the transmission latency period, as shown in the SI. With perfect quarantining, the asymptote $M_p^0(\infty)$ is eventually determined by a cohort that does not include new infections and is thus independent of the transmission delay.

In this work, we have explicitly defined a number of interpretable mathematical metrics that represent the probability of dying from a disease. By rigorously defining these metrics, we are able to reveal the inherent assumptions and factors that affect their estimation. Within survival probability and SIR-type models, we explicitly illustrate how physiologically important parameters such as incubation time, death rate, cure rate, and transmissibility influence the temporal evolution and asymptotic values of mortality ratios. We also discussed how statistical factors such as time of testing after infection (τ_1) and testing ratio (f) affect our estimates. In practice, the mortality ratios $M_1(t)$ and $M_p^1(t)$ may provide good estimates of mortality of patients who have tested positive. In addition to our metrics and mathematical models, we emphasize the importance of curating individual cohort data. These data are more directly related to the probability of death $M_1(t)$ and are subject to the fewest confounding factors and statistical uncertainty.

DATA AVAILABILITY

The datasets that we used in this study are stored in the publicly accessible repositories of Refs. [12, 14, 28].

ACKNOWLEDGEMENTS

LB acknowledges financial support from the SNF Early Postdoc.Mobility fellowship on “Multispecies interacting stochastic systems in biology”. The authors also acknowledge financial support from the Army Research Office (W911NF-18-1-0345), the NIH (R01HL146552), and the National Science Foundation (DMS-1814364).

COMPETING INTERESTS

The authors declare no competing interests.

AUTHOR CONTRIBUTIONS

LB and TC developed the analyses and wrote the manuscript. LB and MX analyzed data, performed numerical computations, and edited the manuscript.

-
- [1] Robert Verity, Lucy C. Okell, Ilaria Dorigatti, Peter Winskill, Charles Whittaker, Natsuko Imai, Gina Cuomo-Dannenburg, Hayley Thompson, Patrick G. T. Walker, Han Fu, Amy Dighe, Jamie T Griffin, Marc Baguelin, Sangeeta Bhatia, Adhiratha Boonyasiri, Anne Cori, Zulma Cucunubá, Rich FitzJohn, Katy Gaythorpe, Will Green, Arran Hamlet, Wes Hinsley, Daniel Laydon, Gemma Nedjati-Gilani, Prof Steven Riley, Sabine van Elsland, Erik Volz, Haowei Wang, Yuanrong Wang, Xiaoyue Xi, Christl A. Donnelly, Azra C. Ghani, and Neil M. Ferguson, “Estimates of the severity of coronavirus disease 2019: a model-based analysis,” *The Lancet Infectious Diseases* (2020), 10.1016/S1473-3099(20)30243-7.
 - [2] Tini Garske, Judith Legrand, Christl A Donnelly, Helen Ward, Simon Cauchemez, Christophe Fraser, Neil M Ferguson, and Azra C Ghani, “Assessing the severity of the novel influenza A/H1N1 pandemic,” *BMJ* **339** (2009), 10.1136/bmj.b2840, <https://www.bmj.com/content>.
 - [3] Zhe Xu, Lei Shi, Yijin Wang, Jiyuan Zhang, Lei Huang, Chao Zhang, Shuhong Liu, Peng Zhao, Hongxia Liu, Li Zhu, *et al.*, “Pathological findings of COVID-19 associated with acute respiratory distress syndrome,” *Lancet Resp. Med.* (2020).
 - [4] Zunyou Wu and Jennifer M McGoogan, “Characteristics of and Important Lessons From the Coronavirus Disease 2019 (COVID-19) Outbreak in China: Summary of a Report of 72314 Cases From the Chinese Center for Disease Control and Prevention,” *JAMA* (2020).

- [5] Sung-mok Jung, Andrei R. Akhmetzhanov, Katsuma Hayashi, Natalie M. Linton, Yichi Yang, Baoyin Yuan, Tetsuro Kobayashi, Ryo Kinoshita, and Hiroshi Nishiura, “Real-Time Estimation of the Risk of Death from Novel Coronavirus (COVID-19) Infection: Inference Using Exported Cases,” *Journal of Clinical Medicine* **9** (2020), 10.3390/jcm9020523.
- [6] Mike Famulare, “2019-nCoV: preliminary estimates of the confirmed-case-fatality-ratio and infection-fatality-ratio, and initial pandemic risk assessment,” https://institutefordiseasemodeling.github.io/nCoV-public/analyses/first_adjusted_mortality_estimates_and_risk_assessment/2019-nCoV-preliminary_age_and_time_adjusted_mortality_rates_and_pandemic_risk_assessment.html (2020), accessed: 2020-03-31.
- [7] Jason Oke and Carl Heneghan, “Global Covid-19 Case Fatality Rates: Oxford COVID-19 Evidence Service,” (2020), accessed: 2020-03-27.
- [8] Anastasios Nikolas Angelopoulos, Reese Pathak, Rohit Varma, and Michael I. Jordan, “Identifying and Correcting Bias from Time- and Severity- Dependent Reporting Rates in the Estimation of the COVID-19 Case Fatality Rate,” arXiv:2003.08592v2 (2020).
- [9] K. Mizumoto and G. Chowell, “Estimating risk for death from 2019 novel coronavirus disease, China, January-February 2020,” *Emerging Infectious Diseases* (2020), 10.3201/eid2606.200233.
- [10] Shigui Ruan, “Likelihood of survival of coronavirus disease 2019,” *The Lancet Infectious Diseases* (2020), [https://doi.org/10.1016/S1473-3099\(20\)30257-7](https://doi.org/10.1016/S1473-3099(20)30257-7).
- [11] Piotr Spychalski, Agata Bayska-Spychalska, and Jarek Kobiela, “Estimating case fatality rates of covid-19,” *The Lancet Infectious Diseases* (2020), [https://doi.org/10.1016/S1473-3099\(20\)30246-2](https://doi.org/10.1016/S1473-3099(20)30246-2).
- [12] “COVID-19 statistics,” <https://www.worldometers.info/coronavirus/> (2020), accessed: 2020-02-26.
- [13] AC Ghani, CA Donnelly, DR Cox, JT Griffin, C Fraser, TH Lam, LM Ho, WS Chan, RM Anderson, AJ Hedley, *et al.*, “Methods for estimating the case fatality ratio for a novel, emerging infectious disease,” *Am. J. Epidemiology* **162**, 479–486 (2005).
- [14] Ensheng Dong, Hongru Du, and Lauren Gardner, “An interactive web-based dashboard to track COVID-19 in real time,” *The Lancet Infectious Diseases* (2020).
- [15] Paul SF Yip, KF Lam, Eric HY Lau, Pui-Hing Chau, Kenneth W Tsang, and Anne Chao, “A comparison study of realtime fatality rates: severe acute respiratory syndrome in Hong Kong, Singapore, Taiwan, Toronto and Beijing, China,” *J. Roy. Stat. Soc. A* **168**, 233–243 (2005).
- [16] Paul SF Yip, Eric HY Lau, KF Lam, and Richard M Huggins, “A chain multinomial model for estimating the real-time fatality rate of a disease, with an application to severe acute respiratory syndrome,” *Am. J. Epidemiol.* **161**, 700–706 (2005).
- [17] Lucas Böttcher, Olivia Woolley-Meza, Nuno AM Araújo, Hans J Herrmann, and Dirk Helbing, “Disease-induced resource constraints can trigger explosive epidemics,” *Sci. Rep.* **5**, 1–11 (2015).
- [18] Lucas Böttcher, Olivia Woolley-Meza, Eric Goles, Dirk Helbing, and Hans J Herrmann, “Connectivity disruption sparks explosive epidemic spreading,” *Phys. Rev. E* **93**, 042315 (2016).
- [19] Julien Riou, Anthony Hauser, Michel J Counotte, and Christian L Althaus, “Adjusted age-specific case fatality ratio during the COVID-19 epidemic in Hubei, China, January and February 2020,” medRxiv (2020), 10.1101/2020.03.04.20031104.
- [20] Of course, at the population level, if there are many deaths, medical facilities are stressed which indirectly leads to an increase in death rates.
- [21] Zhou Xu, Shu Li, Shen Tian, Hao Li, and Ling-quan Kong, “Full spectrum of covid-19 severity still being depicted,” *The Lancet* (2020).
- [22] Elisabeth Mahase, “Coronavirus: COVID-19 has killed more people than SARS and MERS combined, despite lower case fatality rate,” (2020).
- [23] World Health Organization, “WHO Director-General’s opening remarks at the media briefing on COVID-19 - 24 February 2020,” <https://www.who.int/dg/speeches/detail/who-director-general-s-opening-remarks-at-the-media-briefing-on-covid-19---24-february-2020> (2020), accessed: 2020-02-28.
- [24] World Health Organization, “WHO Director-General’s opening remarks at the media briefing on COVID-19 - 3 March 2020,” <https://www.who.int/dg/speeches/detail/who-director-general-s-opening-remarks-at-the-media-briefing-on-covid-19---3-march-2020> (2020), accessed: 2020-03-05.
- [25] R. Porcheddu, C. Serra, D. Kelvin, N. Kelvin, and S. Rubino, “Similarity in Case Fatality Rates (CFR) of COVID-19/SARS-COV-2 in Italy and China,” *The Journal of Infection in Developing Countries* **14**, 125–128 (2020).
- [26] Noah C Peeri, Nistha Shrestha, Md Siddikur Rahman, Rafdzah Zaki, Zhengqi Tan, Saana Bibi, Mahdi Baghbanzadeh, Nasrin Aghamohammadi, Wenyi Zhang, and Ubydul Haque, “The SARS, MERS and novel coronavirus (COVID-19) epidemics, the newest and biggest global health threats: what lessons have we learned?” *International Journal of Epidemiology* (2020), 10.1093/ije/dyaa033.
- [27] The timescale of infections are much smaller than the aging process. In other words, the aging process across the disease time scale is negligible and the age-dependent transport terms $\partial P/\partial a$ can be neglected.
- [28] nCoV 2019 Data Working Group, “Epidemiological Data from the nCoV-2019 Outbreak: Early Descriptions from Publicly Available Data,” <http://virological.org/t/epidemiological-data-from-the-ncov-2019-outbreak-early-descriptions-from-publicly-available-data/337> (2020), accessed: 2020-02-26.
- [29] Chih-Cheng Lai, Tzu-Ping Shih, Wen-Chien Ko, Hung-Jen Tang, and Po-Ren Hsueh, “Severe acute respiratory syndrome coronavirus 2 (SARS-CoV-2) and corona virus disease-2019 (COVID-19): the epidemic and the challenges,” *Int. J.*

Antimicrob. Agents , 105924 (2020).

- [30] Matt J Keeling and Pejman Rohani, *Modeling infectious diseases in humans and animals* (Princeton University Press, 2011).
- [31] Lucas Böttcher and Nino Antulov-Fantulin, “Unifying susceptible-infected-recovered processes on networks,” arXiv preprint arXiv:2002.11765 (2020).
- [32] Katherine E Atkins, Natasha S Wenzel, Martial Ndeffo-Mbah, Frederick L Altice, Jeffrey P Townsend, and Alison P Galvani, “Under-reporting and case fatality estimates for emerging epidemics,” *BMJ* **350**, h1115 (2015).
- [33] Joseph T. Wu, Kathy Leung, Mary Bushman, Nishant Kishore, Rene Niehus, Pablo M. de Salazar, Benjamin J. Cowling, Marc Lipsitch, and Gabriel M. Leung, “Estimating clinical severity of COVID-19 from the transmission dynamics in Wuhan, China,” *Nature Medicine* (2020), 10.1038/s41591-020-0822-7.
- [34] A. G. McKendrick, “Applications of mathematics to medical problems,” *Proc. Edinburgh Math. Soc.* **44**, 98–130 (1926).
- [35] T. Chou and C. D. Greenman, “A Hierarchical Kinetic Theory of Birth, Death and Fission in Age-Structured Interacting Populations,” *Journal of Statistical Physics* **164**, 49–76 (2016. PMID: PMC3894939).
- [36] In both the individual model (Eq. (1)) and population models (Eq. (9)), the death and cure rates are insensitive to changes in age a over the time scale of epidemic if it occurs over, say, only 1-2 years. In this limit, we consider only infection-duration dependence in the population dynamics.
- [37] World Health Organization, “Cumulative Number of Reported Probable Cases of Severe Acute Respiratory Syndrome (SARS),” <https://www.who.int/csr/sars/country/en/> (2020), accessed: 2020-03-30.
- [38] Manuel Battagay, Richard Kuehl, Sarah Tschudin-Sutter, Hans H Hirsch, Andreas F Widmer, and Richard A Neher, “2019-novel Coronavirus (2019-nCoV): estimating the case fatality rate—a word of caution,” *Swiss Medical Weekly* **150** (2020).
- [39] Ruiyun Li, Sen Pei, Bin Chen, Yimeng Song, Tao Zhang, Wan Yang, and Jeffrey Shaman, “Substantial undocumented infection facilitates the rapid dissemination of novel coronavirus (SARS-CoV2),” *Science* (2020).
- [40] Camilla Rothe, Mirjam Schunk, Peter Sothmann, Gisela Bretzel, Guenter Froeschl, Claudia Wallrauch, Thorbjörn Zimmer, Verena Thiel, Christian Janke, Wolfgang Guggemos, Michael Seilmaier, Christian Drosten, Patrick Vollmar, Katrin Zwirgmaier, Sabine Zange, Roman Wlifel, and Michael Hoelscher, “Transmission of 2019-nCoV Infection from an Asymptomatic Contact in Germany,” *New England Journal of Medicine* **382**, 970–971 (2020).
- [41] W. H. Press, S. A. Teukolsky, W. T. Vetterling, and B. P. Flannery, *Numerical Recipes: The Art of Scientific Computing* (Cambridge University Press, 2007).

METHODS

Numerical scheme

To numerically solve Eqs. (9) and (10), we use a uniform discretization $\tau_k = k\Delta\tau, k = 0, 1, \dots, K$. A backward difference operator $[I(\tau_k, t) - I(\tau_{k-1}, t)]/(\Delta\tau)$ is used to approximate $\partial_\tau I(\tau, t)$ and a predictor-corrector Euler scheme is used to advance time [41]. Setting the cut-offs $I(-\Delta\tau, t) \equiv 0$ and $I(K\Delta\tau, t) \equiv 0$, the resulting discretized equations for the full SIR model are

$$\begin{aligned}
S(t + \Delta t) &= S(t) - \Delta t S(t) \sum_{k=0}^K \beta(\tau_k, t) I(\tau_k, t) \Delta\tau, \\
\tilde{I}(\tau_k, t) &= I(\tau_k, t) - \Delta t \frac{I(\tau_k, t) - I(\tau_{k-1}, t)}{\Delta\tau} - \Delta t (c(\tau_k, t) + \mu(\tau_k, t)) I(\tau_k, t), \\
I(\tau_k, t + \Delta t) &= I(\tau_k, t) - \frac{\Delta t}{2} \left[\frac{I(\tau_k, t) - I(\tau_{k-1}, t)}{\Delta\tau} + (c(\tau_k, t) + \mu(\tau_k, t)) I(\tau_k, t) \right. \\
&\quad \left. + \frac{\tilde{I}(\tau_k, t) - \tilde{I}(\tau_{k-1}, t)}{\Delta\tau} + (c(\tau_k, t + \Delta t) + \mu(\tau_k, t + \Delta t)) \tilde{I}(\tau_k, t) \right] \\
&\quad + \delta_{k,0} \frac{\Delta t}{\Delta\tau} S(t) \sum_{j=0}^K \beta(\tau_j, t) I(\tau_j, t) \Delta\tau,
\end{aligned} \tag{18}$$

where \tilde{I} is the initial predicted guess, and the last term proportional to $\delta_{k,0}$ encodes the boundary condition Eq. (10). Note that we use $\sum_{k=0}^K \beta(\tau_k, t) I(\tau_k, t) \Delta\tau$ to indicate the numerical evaluation of $\int_0^\infty d\tau' \beta(\tau', t) I(\tau', t)$. Quadrature methods such as Simpson's rule and the trapezoidal rule can be used to approximate the integral more efficiently.

The total deaths, recovereds, and infecteds at time t are found by

$$\begin{aligned}
D_0(m\Delta t) &= \frac{1}{2} \sum_{j=0}^m \sum_{k=0}^K c(k\Delta\tau, j\Delta t) \left[I(k\Delta\tau, j\Delta t) + \tilde{I}(k\Delta\tau, j\Delta t) \right] \Delta\tau \Delta t, \\
R_0(t) &= \frac{1}{2} \sum_{j=0}^m \sum_{k=0}^K \mu(k\Delta\tau, j\Delta t) \left[I(j\Delta\tau, j\Delta t) + \tilde{I}(k\Delta\tau, j\Delta t) \right] \Delta\tau \Delta t, \\
I(m\Delta t) &= \sum_{k=0}^K I(k\Delta\tau, m\Delta t) \Delta\tau,
\end{aligned}$$

with analogous expressions for $D_1(m\Delta t)$ and $R_1(m\Delta t)$. To obtain a stable integration scheme, the time steps Δt and $\Delta\tau$ have to satisfy $\Delta t/(2\Delta\tau) < 1$. In all of our numerical computations, we thus set $\Delta t = 0.002, \Delta\tau = 0.02$, and $K = 10^4$. In the SI, we show additional plots of the magnitude of $I(\tau, t)$ in the $t - \tau$ plane.

Solutions for τ_1 -averaged probabilities

Using the method of characteristics, we find the formal solution to Eq. (1):

$$P(\tau, t|\tau_1) = \delta(\tau - t - \tau_1) e^{-\int_0^t (\mu(\tau-t+s, s|\tau_1) + c(\tau-t+s, s|\tau_1)) ds}, \tag{19}$$

which can be used to construct the death and cure probabilities

$$\begin{aligned}
P_d(t|\tau_1) &= \int_0^t dt' \mu(\tau_1 + t', t') e^{-\int_0^{t'} (\mu(\tau_1+s, s) + c(\tau_1+s, s)) ds} \\
P_r(t|\tau_1) &= \int_0^t dt' c(\tau_1 + t', t') e^{-\int_0^{t'} (\mu(\tau_1+s, s) + c(\tau_1+s, s)) ds}.
\end{aligned} \tag{20}$$

If we now invoke the functional forms of μ and c given in Eq. (4), we find explicitly

$$P_d(\tau, t | \tau_1) = \begin{cases} \frac{\mu_1}{\mu_1 + c} \left(1 - e^{-(\mu_1 + c)t}\right) & \tau > t + \tau_{\text{inc}} \\ 0 & \tau_{\text{inc}} \geq \tau > \tau_1 \\ \frac{\mu_1 e^{-c(\tau_{\text{inc}} - \tau_1)}}{\mu_1 + c} \left(1 - e^{-(\mu_1 + c)(\tau - \tau_{\text{inc}})}\right) & \tau > \tau_{\text{inc}} \geq \tau_1 \end{cases} \quad (21)$$

and

$$P_r(\tau, t | \tau_1) = \begin{cases} \frac{c}{\mu_1 + c} \left(1 - e^{-(\mu_1 + c)t}\right) & \tau > t + \tau_{\text{inc}} \\ 1 - e^{-ct} & \tau_{\text{inc}} \geq \tau > \tau_1 \\ 1 - e^{-c(\tau_{\text{inc}} - \tau_1)} + \frac{ce^{-c(\tau_{\text{inc}} - \tau_1)}}{\mu_1 + c} \left(1 - e^{-(\mu_1 + c)(\tau - \tau_{\text{inc}})}\right) & \tau > \tau_{\text{inc}} \geq \tau_1. \end{cases} \quad (22)$$

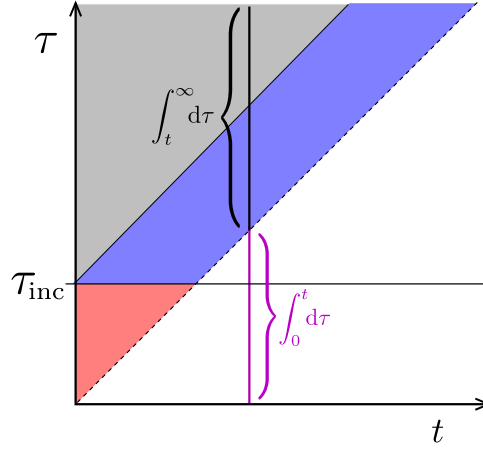


FIG. 5. **Phase plot for $P(\tau > t, t)$ and $I(\tau > t, t)$.** The regions delineating different forms for the solution (Eq. (23)). Here, we have included an incubation time τ_{inc} before which no death occurs. The solution for $\bar{P}(\tau, t)$ or $I(\tau, t)$ in the $\tau < t$ region must be self-consistently solved using the boundary condition Eq. (10). At any fixed time, the integral of $I(\tau, t)$ over $t < \tau \leq \infty$ captures only the initial population, excludes newly infecteds, and is used to compute $D_1(t)$, $R_1(t)$, and $M_p^1(t)$. To compute $D_0(t)$, $R_0(t)$, and $M_p^0(t)$, we integrate across all infecteds (including the integral over $t > \tau \geq 0$ shown in magenta).

Finally, we can also find the τ_1 -averaged probabilities for $\tau \geq t$ by weighting over $\rho(\tau_1; n, \gamma)$. For example,

$$\bar{P}(\tau, t) = \begin{cases} \rho(\tau - t; n, \gamma) e^{-(\mu_1 + c)t} & \tau \geq t + \tau_{\text{inc}} \\ \rho(\tau - t; n, \gamma) e^{-ct} & \tau_{\text{inc}} \geq \tau > t \\ \rho(\tau - t; n, \gamma) e^{-ct} e^{-\mu_1(\tau - \tau_{\text{inc}})} & t + \tau_{\text{inc}} \geq \tau > \tau_{\text{inc}} \end{cases}.$$

These solutions hold for the different regions shown in the phase plot of Fig. 5 and are equivalent to those for $I(\tau > t, t)$. Corresponding expressions for $\bar{P}_d(t)$ and $\bar{P}_r(t)$ can be found and used to construct $M_p^1(t)$. Fig. 6(a) shows the magnitude of $I(\tau, t)$ in the $t - \tau$ plane when we set $S(t) = S$ constant (so that the first equation in Eq. (18) does not apply) such that $\beta_1 S \approx 0.158/\text{day}$. In this case, the epidemic continues to grow in time, but the mortality rates $M_p^{0,1}(t)$ nonetheless converge as $t \rightarrow \infty$. In Fig. 6(b), we set $\beta_1 S = 0$ for $t > t_q$ to model strict quarantining after $t_q = 50$ days. We observe no new infections after the onset of strict quarantine measures. In both cases (quarantine and no quarantine), we use $\rho(\tau; n = 8, \gamma = 1.25)$ (see Eq. (7) in the main text) to describe the initial distribution of infection times τ . As time progresses, more of the distribution of τ moves towards smaller values until quarantine measures take effect (see Fig. 6(c) and (d)).

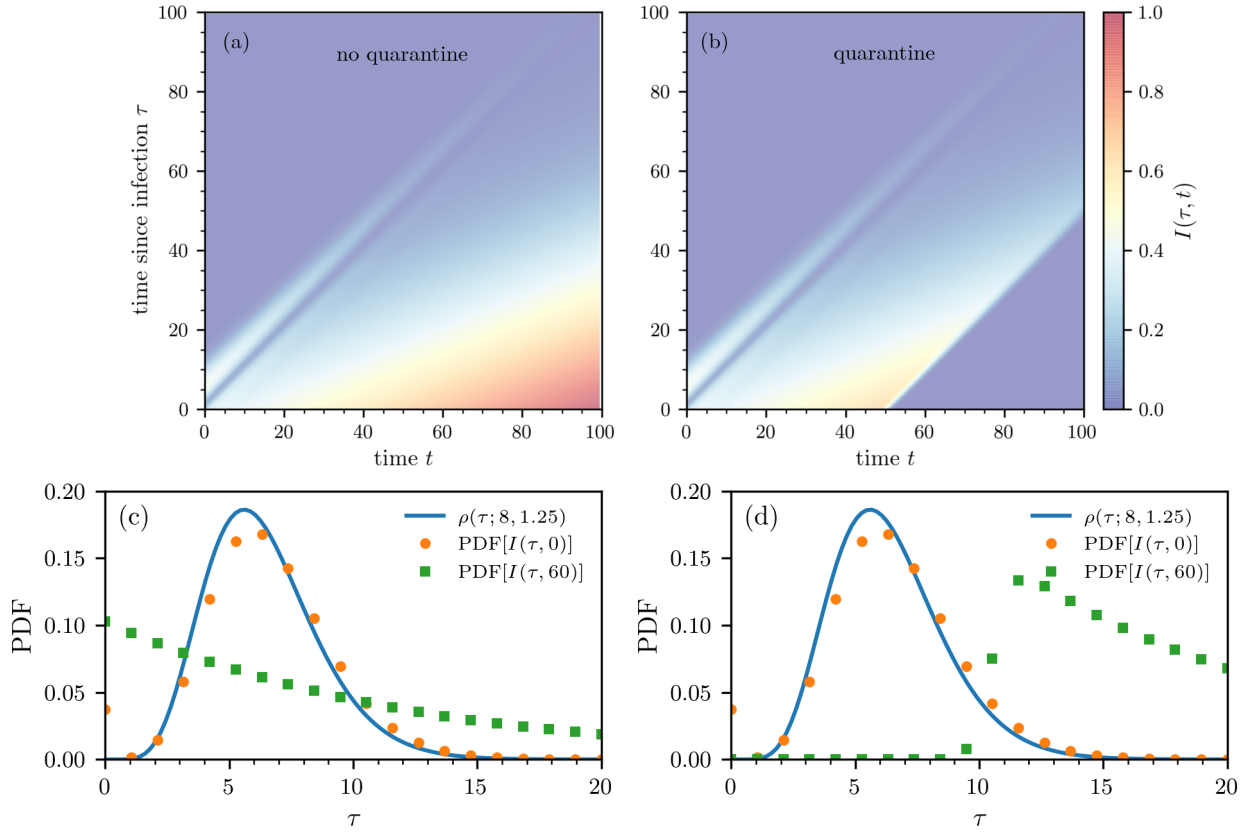


FIG. 6. **Density plots of $I(\tau, t)$ in the $t - \tau$ plane.** Numerical solution of the equation for $I(\tau, t)$ in Eqs. (9) under the assumption of a fixed susceptible size $\beta_1 S = 0.158/\text{day}$. (a) The density without quarantine monotonically grows with time t in the region $\tau < t$ as an unlimited number of susceptibles continually produces infecteds. (b) With quarantining after $t_q = 50$ days, we set $\beta_1 S = 0$ for $t > t_q$, which shuts off new infections. Both plots were generated using the same initial density $\rho(\tau_1)$ defined in Eq. (7). In both cases, the density $I(\tau > t)$ is identical to $P(\tau > t)$ if the same $\rho(\tau_1)$ is used and is independent of disease transmission, susceptible dynamics, etc. (c-d) Probability-density functions (PDFs) of the number of infected $I(\tau, t)$ for $t = 0, 60$ (b) without and (c) with quarantine. The blue solid line corresponds to the initial distribution $\rho(\tau; n = 8, \gamma = 1.25)$ (see Eq. (7)).

SUPPLEMENTARY INFORMATION

Additional examples of mortality-ratio evolutions

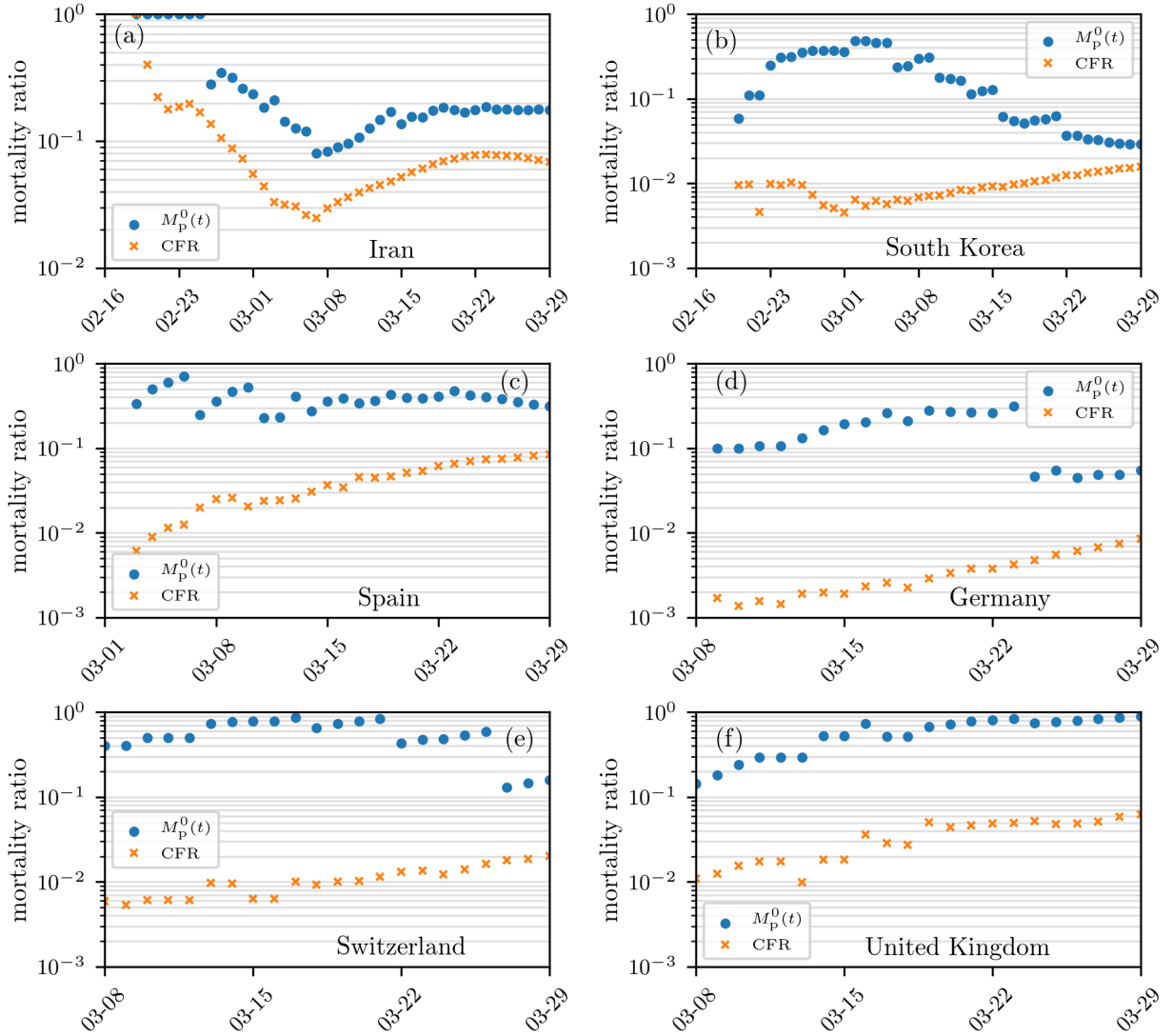


FIG. S1. **Mortality ratio estimates.** Estimates of mortality ratios (see Eqs. (8) and (14) in the main text) of SARS-CoV-2 infections in different countries. The case fatality rate, CFR, corresponds to the number of deaths to date divided by the total number of cases to date. Another population-based mortality ratio is $M_p^0(t)$, the number of deaths divided by the sum of deaths and recovered, up to time t . The data are derived from Ref. [14].

In Fig. S1, we show additional examples of mortality-ratio estimates for Iran, South Korea, Spain, Germany, Switzerland, and the United Kingdom. As in Fig. 1 in the main text, we observe that, by definition, the population-based mortality ratio $M_p^0(t)$ is significantly larger than the corresponding CFR in all cases.

Effects of undertesting

Note that $I(\tau, t)$ in the SIR equations determines the dynamics of the actual infected population. However, (i) typically only a fraction f of the total number of infecteds might be tested and confirmed positive and (ii) the testing of newly infecteds may also be delayed by a distribution $\rho(\tau; n, \gamma)$.

If positive tests represent only a fraction f of the total infected population, and the confirmation of newly infecteds occurs immediately, the known infected density is given by $I^*(\tau, t) = fI(\tau, t)$ where $I(\tau, t)$ is the true total infected population. If testing of newly infecteds occurs after a distribution $\rho(\tau; n, \gamma)$ of infection times, $I^*(\tau, t) = f \int_0^t I(t - \tau + \tau_1, t) \rho(\tau_1; n, \gamma) d\tau_1$.

In our development of $M_p^{0,1}(t)$ and $\text{CFR}_d(t, \tau_{\text{res}})$ in the manuscript, we assumed the entire infected population was tested and confirmed. Thus, $M_p^{0,1}(t)$ and $\text{CFR}_d(t, \tau_{\text{res}})$ were computed using $f = 1$ and more accurately represent the mortality ratios of the population *conditioned* on being tested positive.

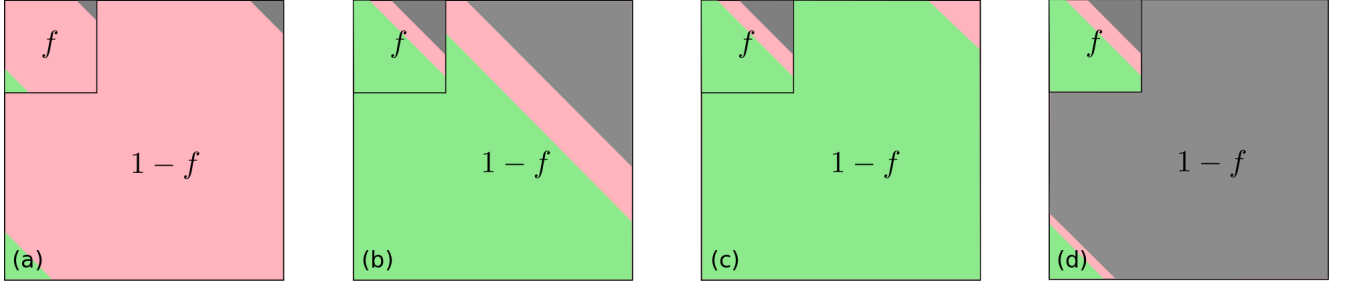


FIG. S2. **Fractional testing.** An example of fractional testing in which a fixed fraction f of the real total infected population is assumed to be tested. The remaining $1 - f$ proportion of infecteds are untested. Equivalently, if the total tested fraction has unit population, then the total population of the untested pool is $1/f - 1$. (a) At short times after an outbreak, most of the infected patients, tested and untested, have not yet resolved (red). Only a small number have died (gray) or have recovered (green). (b) At later times, if the untested population dies at the same rate as the tested population, $M_p(t)$ and CFR remain accurate estimates for the entire infected population. (c) If the untested population is, say, asymptomatic and rarely dies, the true mortality $\mathcal{M}_p^{0,1}(t) \approx fM_p^{0,1}(t)$ is overestimated by the tested mortality $M_p^{0,1}(t)$. (d) Finally, in a scenario in which untested infecteds die at a higher rate than tested ones, $M_p^{0,1}(t)$ and CFR based on the tested fraction *underestimate* the true mortalities.

To estimate the mortality ratio of the population conditioned simply on being infected, we have to estimate the larger number of recovered that went untested. For the most likely scenario in which untested infecteds have negligible death rate, as shown in Fig. S2(c), we can employ the SIR model without death for the untested pool of infecteds,

$$\begin{aligned}
\frac{dS(t)}{dt} &= -S(t) \int_0^\infty d\tau' \beta(\tau', t)(I^*(\tau', t) + I^u(\tau', t)), \\
\frac{\partial I^*(\tau, t)}{\partial t} + \frac{\partial I^*(\tau, t)}{\partial \tau} &= -(\mu(\tau, t) + c(\tau, t))I^*(\tau, t), \\
\frac{\partial I^u(\tau, t)}{\partial t} + \frac{\partial I^u(\tau, t)}{\partial \tau} &= -c(\tau, t)I^u(\tau, t), \\
\frac{dR(t)}{dt} &= \int_0^\infty d\tau c(\tau, t)(I^*(\tau, t) + I^u(\tau, t)),
\end{aligned} \tag{S1}$$

where $I^*(\tau, t) + I^u(\tau, t) = I_T(\tau, t)$, the total density of infecteds, and the production of tested and untested infecteds follow the boundary conditions

$$\begin{aligned}
I^*(0, t) &= fS(t) \int_0^\infty d\tau \beta(\tau, t)I_T(\tau, t) \\
I^u(0, t) &= (1 - f)S(t) \int_0^\infty d\tau \beta(\tau, t)I_T(\tau, t).
\end{aligned} \tag{S2}$$

Here, we have assumed that testing occurs only for the infected who can die. In this scenario, the IFR, or the true CFR of all infecteds, is then $\text{IFR}(t) = D_0^*(t)/N_T(t)$, where in analogy to Eqs. (11) and (12),

$$D_0^*(t) = \int_0^t dt' \int_0^\infty d\tau \mu(\tau, t')I^*(\tau, t'), \quad R_0(t) = \int_0^t dt' \int_0^\infty d\tau c(\tau, t')I_T(\tau, t'), \tag{S3}$$

and

$$N_T(t) = D_0^*(t) + R_0(t) + \int_0^\infty d\tau I_T(\tau, t). \tag{S4}$$

The true mortality ratio is also straightforwardly defined by, for example,

$$\mathcal{M}_p^0(t) = \frac{D_0^*}{D_0^*(t) + R_0^*(t) + R_0^u(t)}, \quad (\text{S5})$$

where

$$R_0^*(t) = \int_0^\infty d\tau \int_0^t dt' c(\tau, t') I^*(\tau, t') \quad \text{and} \quad R_0^u(t) = \int_0^\infty d\tau \int_0^t dt' c(\tau, t') I^u(\tau, t'), \quad (\text{S6})$$

with analogous expressions for $D_1^*(t)$, $R_1^*(t)$, and $R_1^u(t)$. At long times, after resolution of all infecteds, the untested recovered population is

$$R_{0,1}^u(\infty) = \left(\frac{1}{f} - 1\right) (D_{0,1}^*(\infty) + R_{0,1}^*(\infty)), \quad (\text{S7})$$

which yields the asymptotic true ratio $\mathcal{M}_p^{0,1}(\infty) = f M_p^{0,1}(\infty)$ as described in the Discussion and Summary. In this simple rescaling to account for untested populations, we have assumed that all deaths come from the tested pool and that the recovery rate c is the same in the tested and untested pools.

Influence of different transmission rates

In Fig. 3 of the main text, we observe that the population-level mortality ratio $M_p^0(t)$ approaches a plateau during the initial exponential growth phase of an epidemic (*i.e.*, for $S(t) \approx S_0$). If the number of new infections decreases (*e.g.*, due to quarantine measures), $M_p^0(t)$ starts growing until it reaches its asymptotic value $M_p^0(\infty)$. Interestingly, the pre-asymptotic values of $M_p^0(t)$ are smaller for larger infection rates β_1 (see Fig. S3(a)). This counter-intuitive effect arises because larger values of β_1 generate relatively larger numbers of new infected which have a lower chance of dying before τ_{inc} (see Eq. (4) in the main text). A similar effect occurs for non-delayed transmission (*i.e.*, $\tau_\beta \approx 0$).

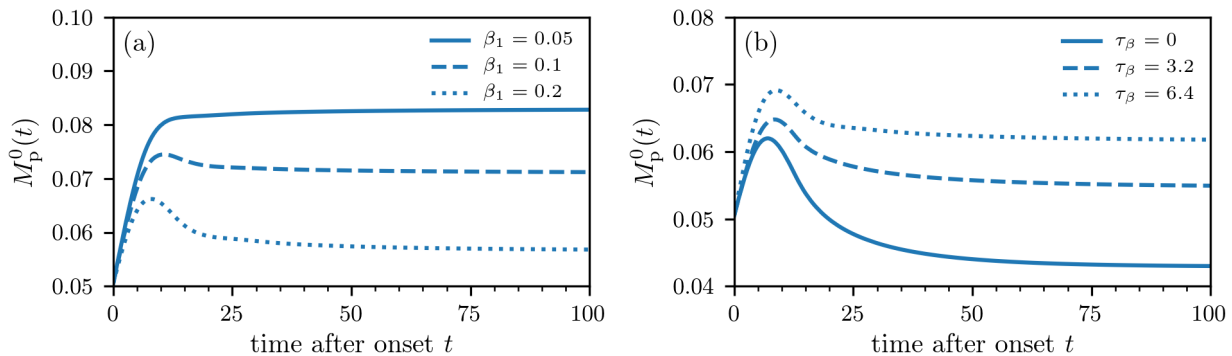


FIG. S3. **Population-level mortality for different infection rates.** (a) The population-level mortality ratio $M_p^0(t)$ for different values of β_1 and an incubation time of $\tau_{\text{inc}} = 6.4$ days. In the initial exponential growth phase of the epidemic (*i.e.*, $S(t) \approx S_0$), larger infection rates β_1 lead to smaller values of $M_p^0(t)$. (b) We observe a similar effect for non-delayed transmissions (*i.e.*, $\tau_\beta \approx 0$). As long as $S(t) \approx S_0$, smaller transmission delays τ_β lead to larger relative numbers of new infections and smaller $M_p^0(t)$.

As the transmission delay decreases, more secondary cases will result from one infection, leading to smaller values of $M_p^0(t)$ in the initial exponential growth phase of an epidemic (see Fig. S3(b)).